Atmosphere Modeling I: Dynamics

Peter Hjort Lauritzen

Atmospheric Modeling & Predictability Section (AMP)
Climate and Global Dynamics Laboratory (CGD)
National Center for Atmospheric Research (NCAR)

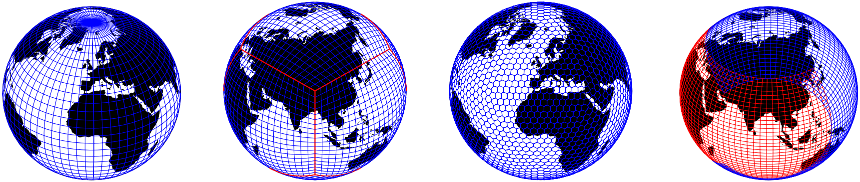

This material is based upon work supported by the NSF National Center for Atmospheric Research, which is a major facility sponsored by the National Science Foundation under Cooperative Agreement No. 1852977.

1. Atmosphere intro
   - Discretization grid: Resolved and un-resolved scales
   - Multi-scale nature of atmosphere dynamics
   - ‘Define’ dynamical core and parameterizations

2. CAM-FV dynamical core (CESM2 ‘work horse’ dynamical core for $\approx 1^\circ$ applications)
   - Horizontal and vertical grid
   - Equations of motion
   - The Lin and Rood (1996) advection scheme
   - Finite-volume discretization of the equations of motion

3. Other dynamical core options in CAM
   - CAM-SE (Spectral-Elements): CESM3 ‘work-horse’ dynamical core
   - CAM-MPAS (Model for Prediction Across Scales): Non-hydrostatic dynamical core being integrated into CESM3

Domain

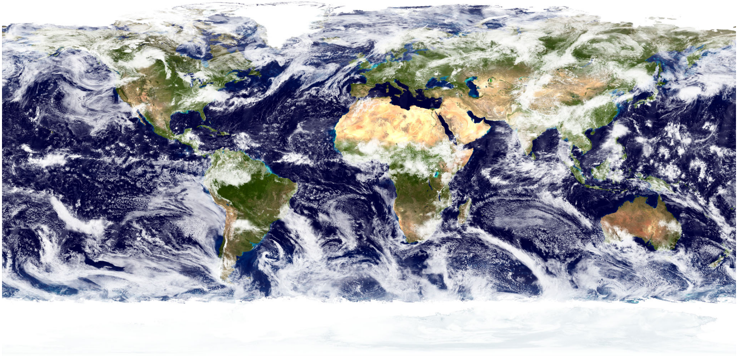

Source: NASA Earth Observatory

Horizontal computational space

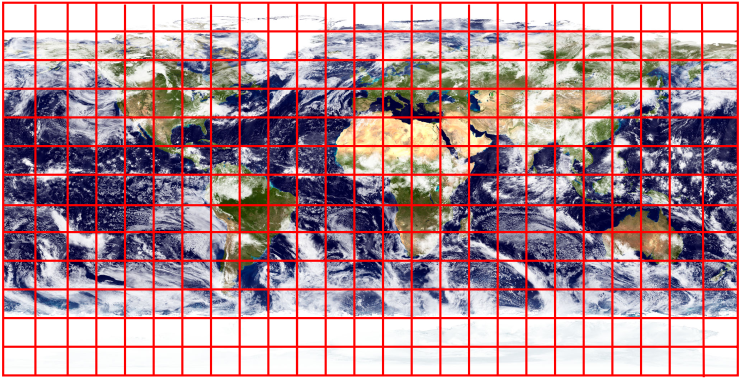

- Red lines: regular latitude-longitude grid
- Grid-cell size defines the smallest scale that can be resolved ($\neq$ **effective resolution!**)
- Many important processes taking place sub-grid-scale that must be parameterized
- Loosely speaking, the parameterizations compute grid-cell average tendencies due to sub-grid-scale processes in terms of the (resolved scale) atmospheric state
- In modeling jargon parameterizations are also referred to as *physics* (what is unphysical about resolved scale dynamics?)

Effective resolution: smallest scale (highest wave-number $k = k_{eff}$) that a model can accurately represent

- k_{eff} can be assessed analytically for linearized equations (Von Neumann analysis)
- In a full model one can assess k_{eff} using total kinetic energy spectra (TKE) of, e.g., horizontal wind $\vec{v}$ (see Figure below)

Effective resolution is typically 4-10 grid-lengths depending on numerical method!
$\Rightarrow$ be careful analyzing phenomena at the grid scale (e.g., extremes)

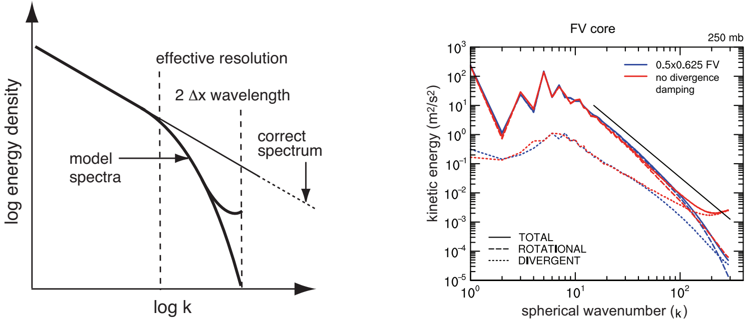

Figure from Skamarock (2011): (left) Schematic depicting the possible behavior of spectral tails derived from model forecasts. (right) TKE (solid lines) as a function of spherical wavenumber for the CCSM finite-volume dynamical core derived from aquaplanet simulations. The total KE is broken into divergent and rotational components (dashed lines) and the solid black lines shows the k^{-3} slope.

Horizontal computational space

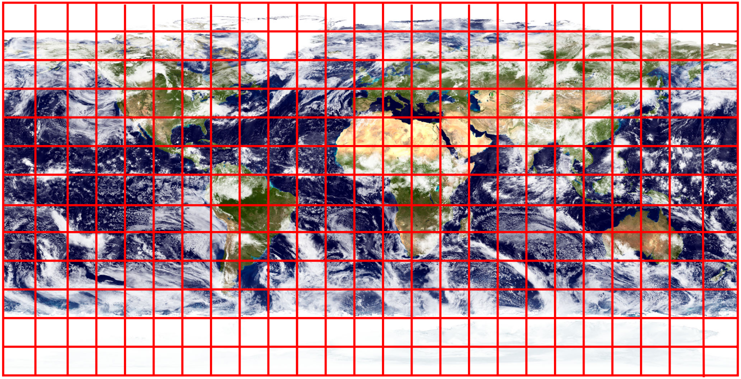

- Red lines: regular latitude-longitude grid
- Grid-cell size defines the smallest scale that can be resolved ($\neq$ **effective resolution!**)
- Many important processes taking place sub-grid-scale that must be parameterized
- Loosely speaking, the parameterizations compute grid-cell average tendencies due to sub-grid-scale processes in terms of the (resolved scale) atmospheric state
- In modeling jargon parameterizations are also referred to as *physics* (what is unphysical about resolved scale dynamics?)

Multi-scale nature of atmosphere dynamics (from Thuburn 2011)

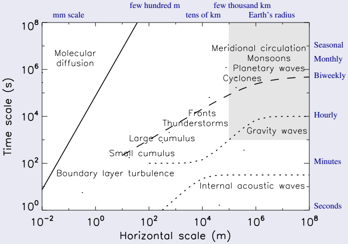

Figure indicates schematically the time scales and horizontal spatial scales of a range of atmospheric phenomena (Figure from Thuburn 2011).

Multi-scale nature of atmosphere dynamics (from Thuburn 2011)

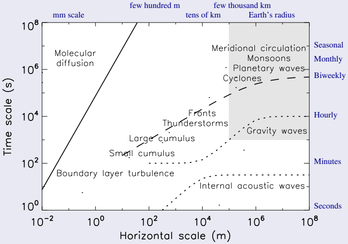

Figure indicates schematically the time scales and horizontal spatial scales of a range of atmospheric phenomena (Figure from Thuburn 2011).

- $\mathcal{O}(10^4 km)$: large scale circulations (Asian summer monsoon).

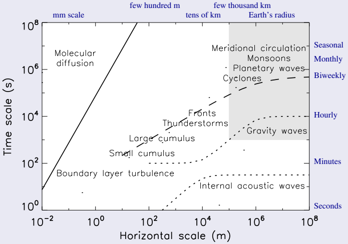

Figure indicates schematically the time scales and horizontal spatial scales of a range of atmospheric phenomena (Figure from Thuburn 2011).

- $\mathcal{O}(10^4 km)$: large scale circulations (Asian summer monsoon).
- $\mathcal{O}(10^4 km)$: undulations in the jet stream and pressure patterns associated with the largest scale Rossby waves (called *planetary waves*)

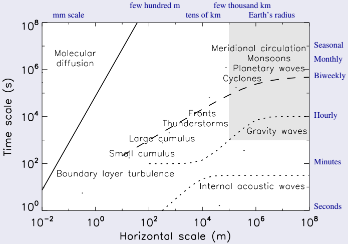

Figure indicates schematically the time scales and horizontal spatial scales of a range of atmospheric phenomena (Figure from Thuburn 2011).

- $\mathcal{O}(10^4 km)$: large scale circulations (Asian summer monsoon).
- $\mathcal{O}(10^4 km)$: undulations in the jet stream and pressure patterns associated with the largest scale Rossby waves (called *planetary waves*)
- $\mathcal{O}(10^3 km)$: cyclones and anticyclones

Multi-scale nature of atmosphere dynamics (from Thuburn 2011)

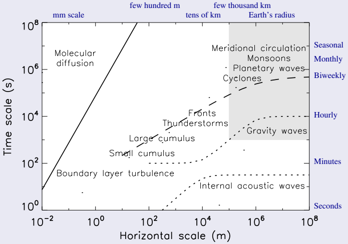

Figure indicates schematically the time scales and horizontal spatial scales of a range of atmospheric phenomena (Figure from Thuburn 2011).

- $\mathcal{O}(10^4 km)$: large scale circulations (Asian summer monsoon).
- $\mathcal{O}(10^4 km)$: undulations in the jet stream and pressure patterns associated with the largest scale Rossby waves (called *planetary waves*)
- $\mathcal{O}(10^3 km)$: cyclones and anticyclones
- $\mathcal{O}(10 km)$: the transition zones between relatively warm and cool air masses can collapse in scale to form fronts with widths of a few tens of km

Multi-scale nature of atmosphere dynamics (from Thuburn 2011)

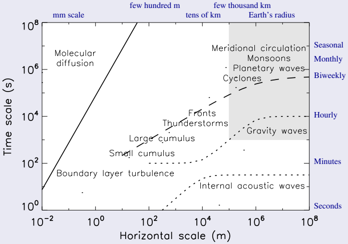

Figure indicates schematically the time scales and horizontal spatial scales of a range of atmospheric phenomena (Figure from Thuburn 2011).

- $\mathcal{O}(10^4 km)$: large scale circulations (Asian summer monsoon).
- $\mathcal{O}(10^4 km)$: undulations in the jet stream and pressure patterns associated with the largest scale Rossby waves (called *planetary waves*)
- $\mathcal{O}(10^3 km)$: cyclones and anticyclones
- $\mathcal{O}(10 km)$: the transition zones between relatively warm and cool air masses can collapse in scale to form fronts with widths of a few tens of km
- $\mathcal{O}(10^3 km - 100m)$: convection can be organized on a huge range of different scales (tropical intraseasonal oscillations; supercell complexes and squall lines; individual small cumulus clouds formed from turbulent boundary layer eddies)

Multi-scale nature of atmosphere dynamics (from Thuburn 2011)

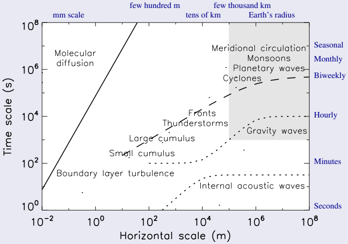

Figure indicates schematically the time scales and horizontal spatial scales of a range of atmospheric phenomena (Figure from Thuburn 2011).

- $\mathcal{O}(10^4 km)$: large scale circulations (Asian summer monsoon).
- $\mathcal{O}(10^4 km)$: undulations in the jet stream and pressure patterns associated with the largest scale Rossby waves (called *planetary waves*)
- $\mathcal{O}(10^3 km)$: cyclones and anticyclones
- $\mathcal{O}(10 km)$: the transition zones between relatively warm and cool air masses can collapse in scale to form fronts with widths of a few tens of km
- $\mathcal{O}(10^3 km - 100 m)$: convection can be organized on a huge range of different scales (tropical intraseasonal oscillations; supercell complexes and squall lines; individual small cumulus clouds formed from turbulent boundary layer eddies)
- $\mathcal{O}(10 m - 1 mm)$: turbulent eddies in boundary layer (lowest few hundred *m*'s of the atmosphere, where the dynamics is dominated by turbulent transports); range in scale from few hundred *m*'s (the boundary layer depth) down to *mm* scale at which molecular diffusion becomes significant.

Multi-scale nature of atmosphere dynamics (from Thuburn 2011)

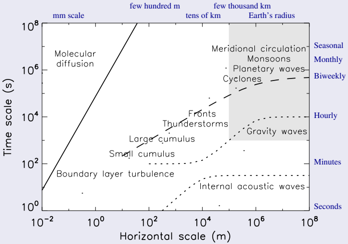

- All of the phenomena along the dashed line are important for weather and climate, and so need to be represented in numerical models.
- Important phenomena occur at all scales - there is no significant *spectral gap*! Moreover, there are strong interactions between the phenomena at different scales, and these interactions need to be represented.
- The lack of any spectral gap makes the modeling of weather/climate very challenging
- The emphasis in this lecture is how we model resolved dynamics; however, it should be borne in mind that equally important is how we represent unresolved processes, and the interactions between resolved and unresolved processes.

- $\mathcal{O}(10^4 km)$: large scale circulations (Asian summer monsoon).
- $\mathcal{O}(10^4 km)$: undulations in the jet stream and pressure patterns associated with the largest scale Rossby waves (called *planetary waves*)
- $\mathcal{O}(10^3 km)$: cyclones and anticyclones
- $\mathcal{O}(10 km)$: the transition zones between relatively warm and cool air masses can collapse in scale to form fronts with widths of a few tens of km
- $\mathcal{O}(10^3 km - 100 m)$: convection can be organized on a huge range of different scales (tropical intraseasonal oscillations; supercell complexes and squall lines; individual small cumulus clouds formed from turbulent boundary layer eddies)
- $\mathcal{O}(10 m - 1 mm)$: turbulent eddies in boundary layer (lowest few hundred *m*'s of the atmosphere, where the dynamics is dominated by turbulent transports); range in scale from few hundred *m*'s (the boundary layer depth) down to *mm* scale at which molecular diffusion becomes significant.

Multi-scale nature of atmosphere dynamics (from Thuburn 2011)

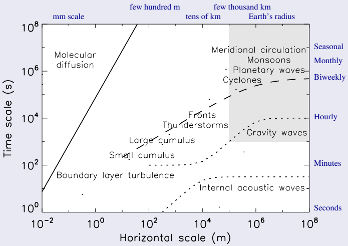

- Two dotted curves correspond to dispersion relations for internal inertio-gravity waves and internal acoustic waves (relatively fast processes)
- these lines lie significantly below the energetically dominant processes on the dashed line
  - $\Rightarrow$ they are energetically weak compared to the dominant processes along the dashed curve
  - $\Rightarrow$ we do relatively little damage if we distort their propagation
  - the fact that these waves are fast puts constraints on the size of Δt (at least for explicit and semi-implicit time-stepping schemes)!

- $\mathcal{O}(10^4 km)$: large scale circulations (Asian summer monsoon).
- $\mathcal{O}(10^4 km)$: undulations in the jet stream and pressure patterns associated with the largest scale Rossby waves (called *planetary waves*)
- $\mathcal{O}(10^3 km)$: cyclones and anticyclones
- $\mathcal{O}(10 km)$: the transition zones between relatively warm and cool air masses can collapse in scale to form fronts with widths of a few tens of km
- $\mathcal{O}(10^3 km - 100 m)$: convection can be organized on a huge range of different scales (tropical intraseasonal oscillations; supercell complexes and squall lines; individual small cumulus clouds formed from turbulent boundary layer eddies)
- $\mathcal{O}(10 m - 1 mm)$: turbulent eddies in boundary layer (lowest few hundred m's of the atmosphere, where the dynamics is dominated by turbulent transports); range in scale from few hundred m's (the boundary layer depth) down to mm scale at which molecular diffusion becomes significant.

Multi-scale nature of atmosphere dynamics (from Thuburn 2011)

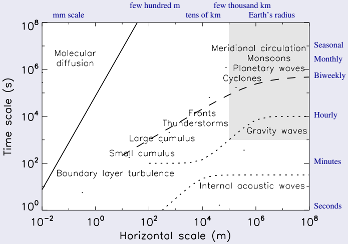

Horizontal resolution:

- the shaded region shows the resolved space/time scales in typical current day climate models (approximately $1^{O} - 2^{O}$ resolution)
- highest resolution at which uniform resolution CAM is run/developed is on the order of $10 - 25km$ (ultra-high resolution 3.75km CAM-MPAS is under development!)
- as the resolution is increased some 'large-scale' parameterizations may no longer be necessary (e.g., large scale convection) and we might need to redesign some parameterizations that were developed for horizontal resolutions of hundreds of km's

- $\mathcal{O}(10^4 km)$: large scale circulations (Asian summer monsoon).
- $\mathcal{O}(10^4 km)$: undulations in the jet stream and pressure patterns associated with the largest scale Rossby waves (called *planetary waves*)
- $\mathcal{O}(10^3 km)$: cyclones and anticyclones
- $\mathcal{O}(10 km)$: the transition zones between relatively warm and cool air masses can collapse in scale to form fronts with widths of a few tens of km
- $\mathcal{O}(10^3 km - 100m)$: convection can be organized on a huge range of different scales (tropical intraseasonal oscillations; supercell complexes and squall lines; individual small cumulus clouds formed from turbulent boundary layer eddies)
- $\mathcal{O}(10m - 1mm)$: turbulent eddies in boundary layer (lowest few hundred *m*'s of the atmosphere, where the dynamics is dominated by turbulent transports); range in scale from few hundred *m*'s (the boundary layer depth) down to *mm* scale at which molecular diffusion becomes significant.

Multi-scale nature of atmosphere dynamics (from Thuburn 2011)

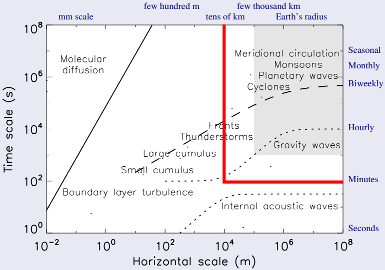

Horizontal resolution:

- the shaded region shows the resolved space/time scales in typical current day climate models (approximately $1^{O} - 2^{O}$ resolution)
- highest resolution at which uniform resolution CAM is run/developed is on the order of $10 - 25km$ (ultra-high resolution 3.75km CAM-MPAS is under development!)
- as the resolution is increased some 'large-scale' parameterizations may no longer be necessary (e.g., large scale convection) and we might need to redesign some parameterizations that were developed for horizontal resolutions of hundreds of km's

- $\mathcal{O}(10^4 km)$: large scale circulations (Asian summer monsoon).
- $\mathcal{O}(10^4 km)$: undulations in the jet stream and pressure patterns associated with the largest scale Rossby waves (called *planetary waves*)
- $\mathcal{O}(10^3 km)$: cyclones and anticyclones
- $\mathcal{O}(10 km)$: the transition zones between relatively warm and cool air masses can collapse in scale to form fronts with widths of a few tens of km
- $\mathcal{O}(10^3 km - 100 m)$: convection can be organized on a huge range of different scales (tropical intraseasonal oscillations; supercell complexes and squall lines; individual small cumulus clouds formed from turbulent boundary layer eddies)
- $\mathcal{O}(10 m - 1 mm)$: turbulent eddies in boundary layer (lowest few hundred m's of the atmosphere, where the dynamics is dominated by turbulent transports); range in scale from few hundred m's (the boundary layer depth) down to mm scale at which molecular diffusion becomes significant.

Model code

Parameterization suite

- Moist processes: deep convection, shallow convection, large-scale condensation
- Radiation and Clouds: cloud microphysics, precipitation processes, radiation
- Turbulent mixing: planetary boundary layer parameterization, vertical diffusion, gravity wave drag

'Resolved' dynamics

'Roughly speaking, the **dynamical core** solves the governing fluid and thermodynamic equations on resolved scales, while the parameterizations represent sub-grid-scale processes and other processes not included in the dynamical core such as radiative transfer.' - Thuburn (2008)

Model code

Parameterization suite

- Moist processes: deep convection, shallow convection, large-scale condensation
- Radiation and Clouds: cloud microphysics, precipitation processes, radiation
- Turbulent mixing: planetary boundary layer parameterization, vertical diffusion, gravity wave drag

Strategies for coupling:

- process-split: dynamical core & parameterization suite are based on the same state and their tendencies are added to produce the updated state (used in CAM-EUL)
- time-split: dynamical core & parameterization suite are calculated sequentially, each based on the state produced by the other (used in CAM-FV; the order matters!).
- different coupling approaches discussed in the context of CCM3 in Williamson (2002)
- simulations are very dependent on coupling time-step (e.g. Williamson and Olson, 2003)
- (re-)emerging research topic: physics-dynamics coupling (PDC) conference series (Gross et al., 2018; Lauritzen et al., 2022)

'Resolved' dynamics

'Roughly speaking, the **dynamical core** solves the governing fluid and thermodynamic equations on resolved scales, while the parameterizations represent sub-grid-scale processes and other processes not included in the dynamical core such as radiative transfer.' - Thuburn (2008)

Spherical (horizontal) discretization grid

CAM-FV uses regular latitude-longitude grid:

- horizontal position: (λ, θ), where λ longitude and θ latitude.
- horizontal resolution specified when creating a new case:

```
./create_newcase -res res ...
```

  where, e.g., res=f09_f09_mg17 which is the $\Delta\lambda \times \Delta\theta = 0.9^\circ \times 1.25^\circ$ horizontal resolution configuration of the FV dynamical core corresponding to nlon=288, nlat=192.

  Changing resolution requires rebuilding (not a namelist variable).

- Note: Convergence of the meridians near the poles.

Vertical coordinate: hybrid sigma ($\sigma = p/p_s$)-pressure (p) coordinate

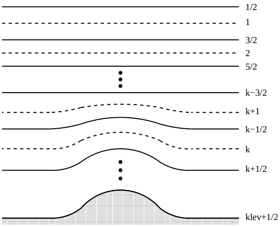

Sigma layers at the bottom (following terrain) with isobaric (pressure) layers aloft.

Pressure at model level interfaces

$$p_{k+1/2} = A_{k+1/2}\, p_0 + B_{k+1/2}\, p_s,$$

where p_s is surface pressure, p_0 is the model top pressure, and $A_{k+1/2}(\in [0:1])$ and $B_{k+1/2}(\in [1:0])$ hybrid coefficients (in model code: *hyai* and *hybi*). Similarly for model level mid-points.

Note: vertical index is 1 at model top and *klev* at surface.

Vertical coordinate

- CAM-FV uses a Lagrangian ('floating') vertical coordinate ξ so that

$$\frac{d\xi}{dt} = 0,$$

i.e. vertical surfaces are material surfaces (no flow across them).

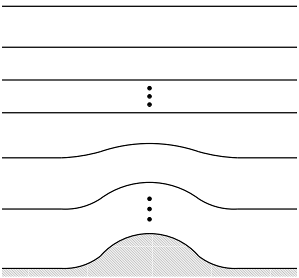

Figure shows 'usual' hybrid $\sigma - p$ vertical coordinate $\eta(p_s, p)$ (where p_s is surface pressure):

- $\eta(p_s, p)$ is a monotonic function of p.
- $\eta(p_s, p_s) = 1$
- $\eta(p_s, 0) = 0$
- $\eta(p_s, p_{top}) = \eta_{top}$.

Boundary conditions are:

- $\frac{d\eta(p_s, p_s)}{dt} = 0$
- $\frac{d\eta(p_s, p_{top})}{dt} = \omega(p_{top}) = 0$

(ω is vertical velocity in pressure coordinates)

- CAM-FV uses a Lagrangian ('floating') vertical coordinate ξ so that

$$\frac{d\xi}{dt} = 0,$$

i.e. vertical surfaces are material surfaces (no flow across them).

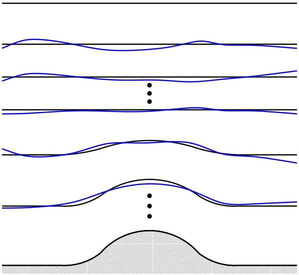

Figure:

- set $\xi = \eta$ at time t_{start} (black lines).
- for $t > t_{start}$ the vertical levels deform as they move with the flow (blue lines).
- to avoid excessive deformation of the vertical levels (non-uniform vertical resolution) the prognostic variables defined in the Lagrangian layers ξ are periodically remapped (= conservative interpolation) back to the Eulerian reference coordinates η (more on this later).

Why use floating Lagrangian vertical coordinates?
Vertical advection terms disappear (3D model becomes 'stacked shallow-water models'; only 2D numerical methods are needed)

Vertical coordinate

The vertical extent is from the surface to

- approximately 42 km's / 2Pa for CAM6
- approximately 140 km's / 10^{-6} hPa for WACCM6 (Whole Atmosphere Community Climate Model)
- approximately 600 km's / 10^{-9} hPa for WACCM-x

Note:

For CAM7 we introduced a mid-top version with 93 levels and model top at 80km in addition to a low-top version with 58 levels and 40km top

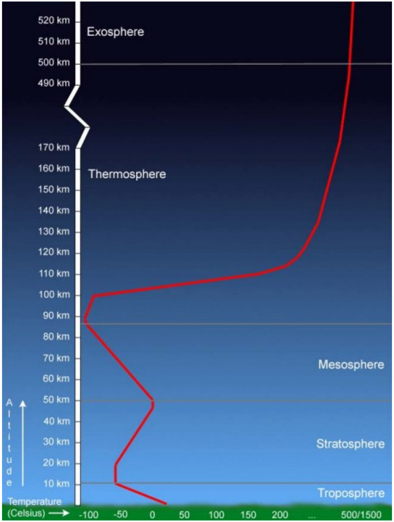

Adiabatic frictionless equations of motion

The following approximations are made to the compressible Euler equations:

- **spherical geoid**: geopotential Φ is only a function of radial distance from the center of the Earth r: $\Phi = \Phi(r)$ (for planet Earth the true gravitational acceleration is much stronger than the centrifugal force).
  $\Rightarrow$ Effective gravity acts only in radial direction

Adiabatic frictionless equations of motion

The following approximations are made to the compressible Euler equations:

- **spherical geoid**: geopotential Φ is only a function of radial distance from the center of the Earth r: $\Phi = \Phi(r)$ (for planet Earth the true gravitational acceleration is much stronger than the centrifugal force).
  $\Rightarrow$ Effective gravity acts only in radial direction
- **quasi-hydrostatic approximation** (also simply referred to as *hydrostatic approximation*): Involves ignoring the acceleration term in the vertical component of the momentum equations so that it reads:
  $$\rho\, g = -\frac{\partial p}{\partial z}, \qquad (1)$$
  where g gravity, ρ density and p pressure. Good approximation down to horizontal scales greater than approximately $10km$.

Adiabatic frictionless equations of motion

The following approximations are made to the compressible Euler equations:

- **spherical geoid**: geopotential Φ is only a function of radial distance from the center of the Earth r: $\Phi = \Phi(r)$ (for planet Earth the true gravitational acceleration is much stronger than the centrifugal force).
  $\Rightarrow$ Effective gravity acts only in radial direction
- **quasi-hydrostatic approximation** (also simply referred to as *hydrostatic approximation*): Involves ignoring the acceleration term in the vertical component of the momentum equations so that it reads:
  $$\rho\, g = -\frac{\partial p}{\partial z}, \qquad (1)$$
  where g gravity, ρ density and p pressure. Good approximation down to horizontal scales greater than approximately $10km$.
- **shallow atmosphere**: a collection of approximations. Coriolis terms involving the horizontal components of Ω are neglected (Ω is angular velocity), factors $1/r$ are replaced with $1/a$ where a is the mean radius of the Earth and certain other metric terms are neglected so that the system retains conservation laws for energy and angular momentum.

Adiabatic frictionless equations of motion using Lagrangian vertical coordinates

Assuming a Lagrangian vertical coordinate the hydrostatic equations of motion integrated over a layer can be written as

$$
\begin{aligned}
\text{mass air:} \quad & \frac{\partial(\delta p)}{\partial t} = -\nabla_h \cdot (\vec{v}_h \delta p)\,, \\
\text{mass tracers:} \quad & \frac{\partial(\delta p q)}{\partial t} = -\nabla_h \cdot (\vec{v}_h\, q \delta p)\,, \\
\text{horizontal momentum:} \quad & \frac{\partial \vec{v}_h}{\partial t} = -\,(\zeta + f)\, \vec{k} \times \vec{v}_h - \nabla_h \kappa - \nabla_p \Phi, \\
\text{thermodynamic:} \quad & \frac{\partial(\delta p \Theta)}{\partial t} = -\nabla_h \cdot (\vec{v}_h \delta p \Theta)
\end{aligned}
$$

where δp is the layer thickness, $\vec{v}_h$ is horizontal wind, q tracer mixing ratio, ζ vorticity, f Coriolis, κ kinetic energy, Θ potential temperature. The momentum equations are written in vector invariant form.

Adiabatic frictionless equations of motion using Lagrangian vertical coordinates

Assuming a Lagrangian vertical coordinate the hydrostatic equations of motion integrated over a layer can be written as

$$
\begin{aligned}
\text{mass air:} \quad & \frac{\partial(\delta p)}{\partial t} = -\nabla_h \cdot (\vec{v}_h \delta p)\,, \\
\text{mass tracers:} \quad & \frac{\partial(\delta p q)}{\partial t} = -\nabla_h \cdot (\vec{v}_h\, q \delta p)\,, \\
\text{horizontal momentum:} \quad & \frac{\partial \vec{v}_h}{\partial t} = -\,(\zeta + f)\,\vec{k} \times \vec{v}_h - \nabla_h \kappa - \nabla_p \Phi, \\
\text{thermodynamic:} \quad & \frac{\partial(\delta p \Theta)}{\partial t} = -\nabla_h \cdot (\vec{v}_h \delta p \Theta)
\end{aligned}
$$

The equations of motion are discretized using an Eulerian finite-volume approach.

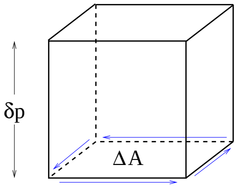

Integrate the flux-form continuity equation horizontally over a control volume:

$$\frac{\partial}{\partial t}\iint_A \delta p \, dA = -\iint_A \nabla_h \left(\vec{v}_h \delta p\right) \, dA, \tag{2}$$

where A is the horizontal extent of the control volume. Using Gauss's divergence theorem for the right-hand side of (2) we get:

$$\frac{\partial}{\partial t}\iint_A \delta p \, dA = -\oint_{\partial A} \delta p \, \vec{v} \cdot \vec{n} \, dA, \tag{3}$$

where ∂A is the boundary of A and $\vec{n}$ is outward pointing normal unit vector of ∂A.

Finite-volume discretization of continuity equation

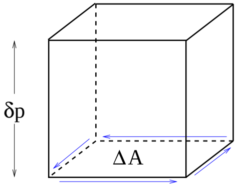

Integrate the flux-form continuity equation horizontally over a control volume:

$$\frac{\partial}{\partial t}\iint_A \delta p\, dA = -\iint_A \nabla_h \left(\vec{v}_h \delta p\right)\, dA, \quad (2)$$

where A is the horizontal extent of the control volume. Using Gauss's divergence theorem for the right-hand side of (2) we get:

$$\frac{\partial}{\partial t}\iint_A \delta p\, dA = -\oint_{\partial A} \delta p\, \vec{v}\cdot\vec{n}\, dA, \quad (3)$$

Right-hand side of (3) represents the instantaneous flux of mass through the vertical faces of the control volume.

Next: integrate over one time-step Δt_{dyn} and discretize left-hand side.

Finite-volume discretization of continuity equation

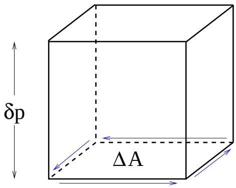

Integrate the flux-form continuity equation horizontally over a control volume:

$$\frac{\partial}{\partial t}\iint_A \delta p \, dA = -\iint_A \nabla_h \left(\vec{v}_h \delta p\right) \, dA, \tag{2}$$

$$\Delta A \, \overline{\delta p}^{\,n+1} - \Delta A \, \overline{\delta p}^{\,n} = -\Delta t_{dyn} \int_{t=n\Delta t}^{t=(n+1)\Delta t} \left[\oint_{\partial A} \delta p \, \vec{v} \cdot \vec{n} \, dA \right] dt, \tag{3}$$

where n is time-level index and $\overline{(\cdot)}$ is cell-averaged value.

The right-hand side represents the mass transported through all of the four vertical control volume faces into the cell during one time-step. Graphical illustration on next slide!

Finite-volume discretization of continuity equation: Tracking mass

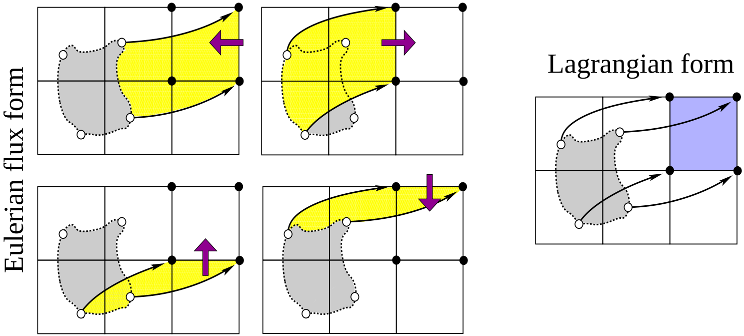

The yellow areas are 'swept' through the control volume faces during one time-step. The grey area is the corresponding Lagrangian area (area moving with the flow with no flow through its boundaries that ends up at the Eulerian control volume after one time-step). Black arrows show parcel trajectories.

Note **equivalence** between Eulerian flux-form and Lagrangian form!

(Lauritzen et al., 2011b)

Finite-volume discretization of continuity equation: Tracking mass

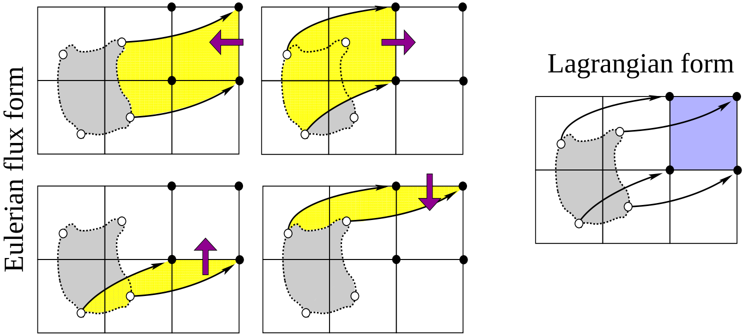

Until now everything has been exact. How do we approximate the fluxes numerically?

- In CAM-FV the Lin and Rood (1996) scheme is used which is a dimensionally split scheme (that is, rather than ‘explicitly’ estimating the boundaries of the yellow areas and integrate over them, fluxes are estimated by successive applications of one-dimensional operators in each coordinate direction).

$$\overline{\delta p}^{n+1} = \overline{\delta p}^{n} + F^{\lambda}\left[\frac{1}{2}\left(\overline{\delta p}^{n} + f^{\theta}(\overline{\delta p}^{n})\right)\right] + F^{\theta}\left[\frac{1}{2}\left(\overline{\delta p}^{n} + f^{\lambda}(\overline{\delta p}^{n})\right)\right],$$

where

$$F^{\lambda,\theta} = \text{ flux divergence in } \lambda \text{ or } \theta \text{ coordinate direction}$$
$$f^{\lambda,\theta} = \text{ advective update in } \lambda \text{ or } \theta \text{ coordinate direction}$$

Adiabatic frictionless equations of motion

Hydrostatic equations of motion integrated over a Lagrangian layer

$$\frac{\partial(\delta p)}{\partial t} = -\nabla_h \cdot (\vec{v}_h \delta p)\,,$$
$$\frac{\partial(\delta p q)}{\partial t} = -\nabla_h \cdot (\vec{v}_h \delta p)\,,$$
$$\frac{\partial \vec{v}_h}{\partial t} = -(\zeta + f)\,\vec{k} \times \vec{v}_h - \nabla_h \kappa - \nabla_p \Phi,$$
$$\frac{\partial(\delta p \Theta)}{\partial t} = -\nabla_h \cdot (\vec{v}_h \delta p \Theta)$$

The equations of motion are discretized using an Eulerian finite-volume approach.

Adiabatic frictionless equations of motion

Hydrostatic equations of motion integrated over a Lagrangian layer

$$
\begin{aligned}
\overline{\delta p}^{n+1} &= \overline{\delta p}^{n} + F^{\lambda}\left[\frac{1}{2}\left(\overline{\delta p}^{n} + f^{\theta}(\overline{\delta p}^{n})\right)\right] + F^{\theta}\left[\frac{1}{2}\left(\overline{\delta p}^{n} + f^{\lambda}(\overline{\delta p}^{n})\right)\right], \\
\frac{\partial(\delta p q)}{\partial t} &= -\nabla_h \cdot (\vec{v}_h \delta p), \\
\frac{\partial \vec{v}_h}{\partial t} &= -(\zeta + f)\,\vec{k} \times \vec{v}_h - \nabla_h \kappa - \nabla_p \Phi, \\
\frac{\partial(\delta p \Theta)}{\partial t} &= -\nabla_h \cdot (\vec{v}_h \delta p \Theta)
\end{aligned}
$$

Adiabatic frictionless equations of motion

Hydrostatic equations of motion integrated over a Lagrangian layer

$$
\begin{aligned}
\overline{\delta p}^{n+1} &= \overline{\delta p}^{n} + F^{\lambda}\left[\frac{1}{2}\left(\overline{\delta p}^{n} + f^{\theta}(\overline{\delta p}^{n})\right)\right] + F^{\theta}\left[\frac{1}{2}\left(\overline{\delta p}^{n} + f^{\lambda}(\overline{\delta p}^{n})\right)\right],\\
\overline{\delta p q}^{n+1} &= \text{super-cycled},\\
\frac{\partial \vec{v}_h}{\partial t} &= -\left(\zeta + f\right)\vec{k} \times \vec{v}_h - \nabla_h \kappa - \nabla_p \Phi,\\
\frac{\partial(\delta p \Theta)}{\partial t} &= -\nabla_h \cdot (\vec{v}_h \delta p \Theta)
\end{aligned}
$$

Adiabatic frictionless equations of motion

Hydrostatic equations of motion integrated over a Lagrangian layer

$$
\begin{aligned}
\overline{\delta p}^{n+1} &= \overline{\delta p}^{n} + F^{\lambda}\left[\frac{1}{2}\left(\overline{\delta p}^{n} + f^{\theta}(\overline{\delta p}^{n})\right)\right] + F^{\theta}\left[\frac{1}{2}\left(\overline{\delta p}^{n} + f^{\lambda}(\overline{\delta p}^{n})\right)\right],\\
\overline{\delta pq}^{n+1} &= \text{super-cycled},\\
\vec{v}_h^{n+1} &= \vec{v}_h^{n} - \vec{\Gamma}^{1}\left[(\zeta + f)\,\vec{k} \times \vec{v}_h\right] - \nabla_h\left(\vec{\Gamma}^{2}\kappa\right) - \Delta t_{dyn}\widehat{P},\\
\frac{\partial(\delta p\Theta)}{\partial t} &= -\nabla_h \cdot (\vec{v}_h \delta p \Theta)
\end{aligned}
$$

- $\vec{\Gamma}^1$ is operator using combinations of $F^{\lambda,\theta}$ and $f^{\lambda,\theta}$ as components to approximate the time-volume-average of the vertical component of absolute vorticity. Similarly for $\vec{\Gamma}^2$ but for kinetic energy. ∇_h is simply approximated by finite differences. For details see Lin (2004).
- $\widehat{P}$ is a finite-volume discretization of the pressure gradient force (see Lin 1997 for details).

Adiabatic frictionless equations of motion

Hydrostatic equations of motion integrated over a Lagrangian layer

$$
\begin{aligned}
\overline{\delta p}^{n+1} &= \overline{\delta p}^{n} + F^{\lambda}\left[\frac{1}{2}\left(\overline{\delta p}^{n} + f^{\theta}(\overline{\delta p}^{n})\right)\right] + F^{\theta}\left[\frac{1}{2}\left(\overline{\delta p}^{n} + f^{\lambda}(\overline{\delta p}^{n})\right)\right], \\
\overline{\delta pq}^{n+1} &= \text{super-cycled}, \\
\vec{v}_h^{n+1} &= \vec{v}_h^{n} - \vec{\Gamma}^{1}\left[(\zeta + f)\,\vec{k}\times\vec{v}_h\right] - \nabla_h\left(\vec{\Gamma}^{2}\kappa\right) - \Delta t_{dyn}\widehat{P}, \\
\overline{\Theta\delta p}^{n+1} &= \overline{\Theta\delta p}^{n} + F^{\lambda}\left[\frac{1}{2}\left(\overline{\Theta\delta p}^{n} + f^{\theta}(\overline{\Theta\delta p}^{n})\right)\right] + F^{\theta}\left[\frac{1}{2}\left(\overline{\Theta\delta p}^{n} + f^{\lambda}(\overline{\Theta\delta p}^{n})\right)\right],
\end{aligned}
$$

Adiabatic frictionless equations of motion

Hydrostatic equations of motion integrated over a Lagrangian layer

$$
\begin{aligned}
\overline{\delta p}^{n+1} &= \overline{\delta p}^{n} + F^{\lambda}\left[\frac{1}{2}\left(\overline{\delta p}^{n} + f^{\theta}(\overline{\delta p}^{n})\right)\right] + F^{\theta}\left[\frac{1}{2}\left(\overline{\delta p}^{n} + f^{\lambda}(\overline{\delta p}^{n})\right)\right],\\
\overline{\delta pq}^{n+1} &= \text{super-cycled},\\
\vec{v}_h^{n+1} &= \vec{v}_h^{n} - \vec{\Gamma}^1\left[(\zeta + f)\,\vec{k}\times\vec{v}_h\right] - \nabla_h\left(\vec{\Gamma}^2\kappa\right) - \Delta t_{dyn}\widehat{P},\\
\overline{\Theta\delta p}^{n+1} &= \overline{\Theta\delta p}^{n} + F^{\lambda}\left[\frac{1}{2}\left(\overline{\Theta\delta p}^{n} + f^{\theta}(\overline{\Theta\delta p}^{n})\right)\right] + F^{\theta}\left[\frac{1}{2}\left(\overline{\Theta\delta p}^{n} + f^{\lambda}(\overline{\Theta\delta p}^{n})\right)\right],
\end{aligned}
$$

- No explicit diffusion operators in equations (so far!).
- Implicit diffusion trough shape-preservation constraints in F and f operators.
- CAM-FV has 'control' over vorticity at the grid scale through implicit diffusion in the operators F and f but it does not have explicit control over divergence near the grid scale.

Adiabatic frictionless equations of motion

Hydrostatic equations of motion integrated over a Lagrangian layer

$$\overline{\delta p}^{n+1} = \overline{\delta p}^{n} + F^{\lambda}\left[\frac{1}{2}\left(\overline{\delta p}^{n} + f^{\theta}(\overline{\delta p}^{n})\right)\right] + F^{\theta}\left[\frac{1}{2}\left(\overline{\delta p}^{n} + f^{\lambda}(\overline{\delta p}^{n})\right)\right],$$

$$\overline{\delta pq}^{n+1} = \text{super-cycled},$$

$$\vec{v}_h^{n+1} = \vec{v}_h^{n} - \vec{\Gamma}^1\left[(\zeta + f)\,\vec{k}\times\vec{v}_h\right] - \nabla_h\left(\vec{\Gamma}^2\kappa\right) - \Delta t_{dyn}\widehat{P} + \Delta t_{dyn}\nabla_h\left(\nu\nabla_h^{\ell}D\right), \ell = 0, 2$$

$$\overline{\Theta\delta p}^{n+1} = \overline{\Theta\delta p}^{n} + F^{\lambda}\left[\frac{1}{2}\left(\overline{\Theta\delta p}^{n} + f^{\theta}(\overline{\Theta\delta p}^{n})\right)\right] + F^{\theta}\left[\frac{1}{2}\left(\overline{\Theta\delta p}^{n} + f^{\lambda}(\overline{\Theta\delta p}^{n})\right)\right],$$

- No explicit diffusion operators in equations.
- Implicit diffusion trough shape-preservation constraints in F and f operators.
- The above discretization leads to 'control' over vorticity at the grid scale through implicit diffusion but no explicit control over divergence.
- Add divergence damping (2^{nd}-order or 4^{th}-order) term to momentum equations.
  Optionally a 'Laplacian-like' damping of wind components is used in upper 3 levels to slow down excessive polar night jet that appears at high horizontal resolutions.
  namelist variable: `fv_div24del2flag`

More details: Lauritzen et al. (2011a); for a stability analysis of divergence damping in CAM see Whitehead et al. (2011)

Total kinetic energy spectra

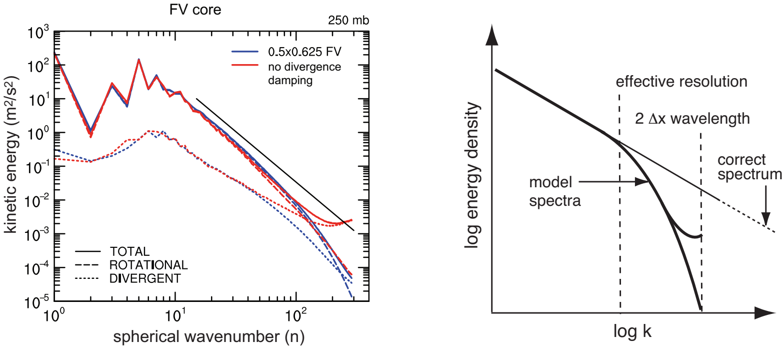

Figure: (left) Solid black line shows k^{-3} slope (courtesy of D.L. Williamson). (right) Schematic of 'effective resolution' (Figure from Skamarock (2011)).

- (left) Without divergence damping there is a spurious accumulation of total kinetic energy associated with divergent modes near the grid scale.
- (right) Note: total kinetic energy spectra can also be used to assess 'effective resolution' (see, e.g., discussion in Skamarock, 2011)

The reformulation of global climate/weather models for massively parallel computer architectures

Traditionally the equations of motion have been discretized on the traditional regular latitude-longitude grid using either

1. spherical harmonics based methods (dominated for over 40 years)
2. finite-difference/finite-volume methods (e.g., CAM-FV)

Both methods require non-local communication:

1. Legendre transform
2. 'polar[a] filters' (due to convergence of the meridians near the poles)

respectively, and are therefore not "trivially" amenable for massively parallel compute systems.

[a] confusing terminology: filters are also applied away from polar regions: $\theta \in [\pm 36^\circ, \pm 90]$

The reformulation of global climate/weather models for massively parallel computer architectures

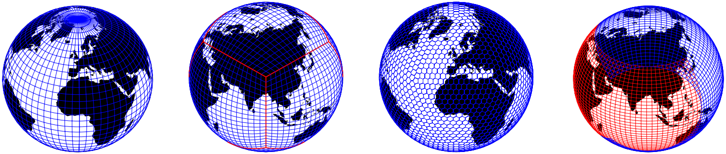

- Quasi-uniform grid + local numerical method ⇒ no non-local communication necessary

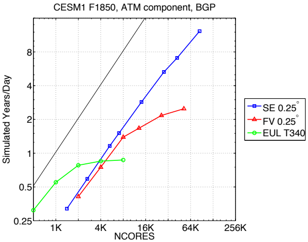

Performance in through-put for different dynamical cores in NCAR's global atmospheric climate model:

horizontal resolution: approximately 25km × 25km grid boxes

- EUL = spectral transform (lat-lon grid)
- FV = finite-volume (reg. lat-lon grid)
- SE = spectral element (cubed-sphere grid)

Computer = Intrepid (IBM Blue Gene/P Solution) at Argonne National Laboratory

Note that for small compute systems CAM-EUL has SUPERIOR throughput!!

- CAM-SE (Lauritzen et al., 2018): Spectral Elements
  - Dynamical core based on HOMME (High-Order Method Modeling Environment, Thomas and Loft 2005).
  - Mass-conservative to machine precision and good total energy conservation properties
  - Conserves axial angular momentum very well (Lauritzen et al., 2014)
  - Discretized on cubed-sphere (uniform resolution or conforming mesh-refinement; Zarzycki et al., 2014) and highly scalable
  - 'Work-horse' for CESM3 climate applications ($1/4^\circ$)
  - New NCAR CAM-SE version using dry-mass vertical coordinates and with comprehensive treatment of condensates and energy released with CESM2
  - Optional transport with finite-volume scheme (Lauritzen et al., 2017) and finite-volume physics grid (Herrington et al., 2018, 2019)

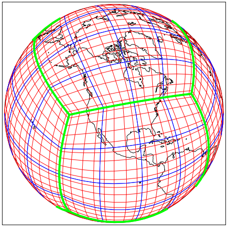

- MPAS (Skamarock et al., 2012): Finite-volume unstructured
  - MPAS = Model for Prediction Across Scales
  - Centroidal Voronoi tessellation of the sphere
  - Fully compressible non-hydrostatic discretization similar to Weather Research Weather (WRF) model (Skamarock and Klemp, 2008)
  - Integrated into CAM but not fully supported yet
  - We are developing ultra-high resolution version of CAM with CAM-MPAS

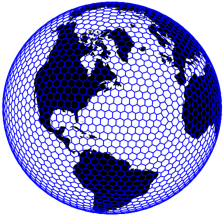

- FV3: Finite-volume
  - 'cubed-sphere' version of CAM-FV `https://www.gfdl.noaa.gov/fv3/fv3-documentation-and-references/`
  - (limited support in CESM)

Upper figures courtesy of R.D. Nair.

Both CAM-SE and MPAS support mesh-refinement:

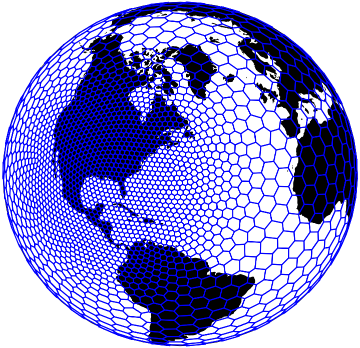

See talk later this week specfically on mesh-refinement applications with CESM!

CAM-SE: (Lauritzen et al., 2018)

CAM-SE uses a continuous Galerkin finite element method (Taylor et al., 1997) referred to as **Spectral Elements (SE)**:

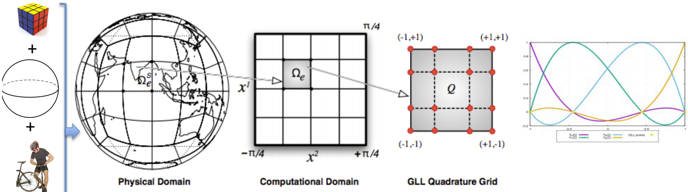

Figures from Nair et al. (2011)

- Physical domain: Tile the sphere with quadrilaterals using the gnomonic cubed-sphere projection
- Computational domain: Mapped local Cartesian domain
- Each element operates with a Gauss-Lobatto-Legendre (GLL) quadrature grid

  Gaussian quadrature using the GLL grid will integrate a polynomial of degree $2N - 1$ exactly, where N is degree of polynomial
- Elementwise the solution is projected onto a tensor product of 1D Legendre basis functions

  by multiplying the equations of motion by test functions; *weak Galerkin formation*

  $\rightarrow$ all derivatives inside each element can be computed analytically!

CAM-SE uses a continuous Galerkin finite element method (Taylor et al., 1997) referred to as **Spectral Elements (SE)**:

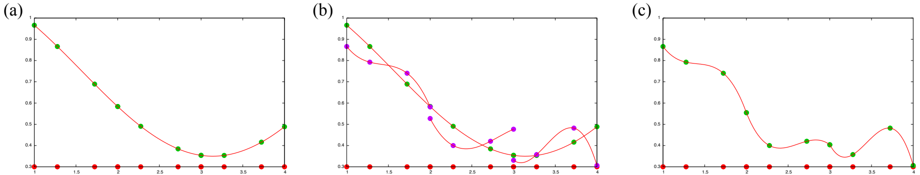

How do solutions in each element 'communicate' with each other?

- The solution is projected onto the space of globally continuous (C^0) piecewise polynomials
- $\rightarrow$ point values are forced to be C^0 continuous along element boundaries by averaging.
- Note: this is the only operation in which information 'propagates' between elements
- MPI data-communication: only information on the boundary of elements!
- For more details see explanation/discussion in Herrington et al. (2018).

CAM-SE-CSLAM (Herrington et al., 2018, 2019)

CAM-SE has the option to run physics on a finite-volume grid that is coarser, same or finer resolution compared to the dynamics grid. This configuration uses inherently conservative CSLAM (Conservative Semi-LAgrangan Multi-tracer) transport scheme (Lauritzen et al., 2017).

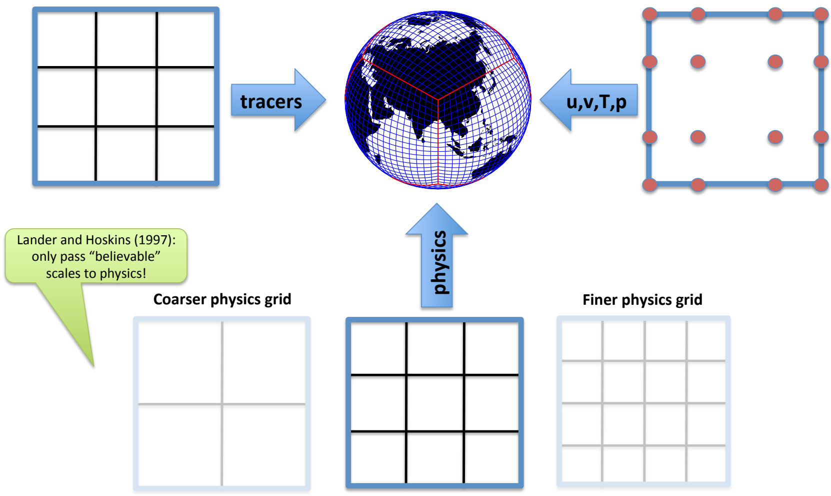

Interested in numerical methods for global models?

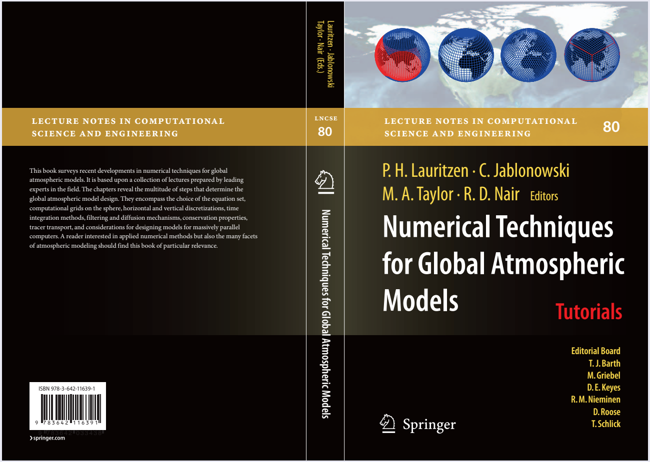

- Book based on the lectures given at the 2008 NCAR ASP (Advance Study Program) Summer Colloquium.
- 16 Chapters; authors include J.Thuburn, J.Tribbia, D.Durran, T.Ringler, W.Skamarock, R.Rood, J.Dennis, Editors, ... Foreword by D. Randall
- More details at: http://www.cgd.ucar.edu/cms/pel/colloquium.html and http://www.cgd.ucar.edu/cms/pel/lncse.html

Questions? Contact pel@ucar.edu

Adcroft, A., Hill, C., and Marshall, J. (1997). Representation of topography by shaved cells in a height coordinate ocean model. *Mon. Wea. Rev.*, 125(9):2293–2315.

Gross, M., Wan, H., Rasch, P. J., Caldwell, P. M., Williamson, D. L., Klocke, D., Jablonowski, C., Thatcher, D. R., Wood, N., Cullen, M., Beare, B., Willett, M., Lemarié, F., Blayo, E., Malardel, S., Termonia, P., Gassmann, A., Lauritzen, P. H., Johansen, H., Zarzycki, C. M., Sakaguchi, K., and Leung, R. (2018). Physics-dynamics coupling in weather, climate and earth system models: Challenges and recent progress. *Mon. Wea. Rev.*, 146:3505–3544.

Herrington, A. R., Lauritzen, P. H., Reed, K. A., Goldhaber, S., and Eaton, B. E. (2019). Exploring a lower-resolution physics grid in CAM-SE-CSLAM. *J. Adv. Model. Earth Syst.*, page 1894– 1916.

Herrington, A. R., Lauritzen, P. H., Taylor, M. A., Goldhaber, S., Eaton, B. E., Reed, K. A., and Ullrich, P. A. (2018). Physics-dynamics coupling with element-based high-order Galerkin methods: quasi equal-area physics grid. *Mon. Wea. Rev.*, 134:3610–3624.

Kasahara, A. (1974). Various vertical coordinate systems used for numerical weather prediction. *Mon. Wea. Rev.*, 102(7):509–522.

Lauritzen, P. H., Bacmeister, J. T., Dubos, T., Lebonnois, S., and Taylor, M. A. (2014). Held-Suarez simulations with the Community Atmosphere Model Spectral Element (CAM-SE) dynamical core: A global axial angular momentum analysis using Eulerian and floating Lagrangian vertical coordinates. *J. Adv. Model. Earth Syst.*, 6.

Lauritzen, P. H., Kevlahan, N. K.-R., Toniazzo, T., Eldred, C., Dubos, T., Gassmann, A., Larson, V. E., Jablonowski, C., Guba, O., Shipway, B., Harrop, B. E., Lemari¡C3¿¡A9¿, F., Tailleux, R., Herrington, A. R., Large, W., Rasch, P. J., Donahue, A. S., Wan, H., Conley, A., and Bacmeister, J. T. (2022). Reconciling and improving formulations for thermodynamics and conservation principles in earth system models (esms). *J. Adv. Model. Earth Syst.*, 14(9):e2022MS003117. e2022MS003117 2022MS003117.

Lauritzen, P. H., Mirin, A., Truesdale, J., Raeder, K., Anderson, J., Bacmeister, J., and Neale, R. B. (2011a). Implementation of new diffusion/filtering operators in the CAM-FV dynamical core. *Int. J. High Perform. Comput. Appl.*

Lauritzen, P. H., Nair, R., Herrington, A., Callaghan, P., Goldhaber, S., Dennis, J., Bacmeister, J. T., Eaton, B., Zarzycki, C., Taylor, M. A., Gettelman, A., Neale, R., Dobbins, B., Reed, K., and Dubos, T. (2018). NCAR release of CAM-SE in CESM2.0: A reformulation of the spectral-element dynamical core in dry-mass vertical coordinates with comprehensive treatment of condensates and energy. *J. Adv. Model. Earth Syst.*, 10(7):1537–1570.

Lauritzen, P. H., Taylor, M. A., Overfelt, J., Ullrich, P. A., Nair, R. D., Goldhaber, S., and Kelly, R. (2017). CAM-SE-CSLAM: Consistent coupling of a conservative semi-lagrangian finite-volume method with spectral element dynamics. *Mon. Wea. Rev.*, 145(3):833–855.

Lauritzen, P. H., Ullrich, P. A., and Nair, R. D. (2011b). Atmospheric transport schemes: desirable properties and a semi-Lagrangian view on finite-volume discretizations, in: P.H. Lauritzen, R.D. Nair, C. Jablonowski, M. Taylor (Eds.), Numerical techniques for global atmospheric models. *Lecture Notes in Computational Science and Engineering, Springer, 2011*, 80.

Lin, S. J. (1997). Ti: A finite-volume integration method for computing pressure gradient force in general vertical coordinates. *Quart. J. Roy. Meteor. Soc.*, 123:1749–1762.

Lin, S.-J. (2004). A 'vertically Lagrangian' finite-volume dynamical core for global models. *Mon. Wea. Rev.*, 132:2293–2307.

Lin, S. J. and Rood, R. B. (1996). Multidimensional flux-form semi-Lagrangian transport schemes. *Mon. Wea. Rev.*, 124:2046–2070.

Schär, C., Leuenberger, D., Fuhrer, O., Lüthi, D., and Girard, C. (2002). A new terrain-following vertical coordinate formulation for atmospheric prediction models. *Mon. Wea. Rev.*, 130(10):2459–2480.

Skamarock, W. (2011). Kinetic energy spectra and model filters, in: P.H. Lauritzen, R.D. Nair, C. Jablonowski, M. Taylor (Eds.), Numerical techniques for global atmospheric models. *Lecture Notes in Computational Science and Engineering, Springer*, 80.

Skamarock, W. C. and Klemp, J. B. (2008). A time-split nonhydrostatic atmospheric model for weather research and forecasting applications. *J. Comput. Phys.*, 227:3465–3485.

Skamarock, W. C., Klemp, J. B., Duda, M. G., Fowler, L. D., Park, S.-H., and Ringler, T. D. (2012). A multiscale nonhydrostatic atmospheric model using centroidal Voronoi tesselations and C-grid staggering. *Mon. Wea. Rev.*, 140:3090–3105.

Taylor, M. A., Tribbia, J., and Iskandarani, M. (1997). The spectral element method for the shallow water equations on the sphere. *J. Comput. Phys.*, 130:92–108.

Thomas, S. J. and Loft, R. D. (2005). The NCAR spectral element climate dynamical core: Semi-implicit Eulerian formulation. *J. Sci. Comput.*, 25:307–322.

Thuburn, J. (2008). Some conservation issues for the dynamical cores of NWP and climate models. *J. Comput. Phys.*, 227:3715–3730.

Thuburn, J. (2011). Some basic dynamics relevant to the design of atmospheric model dynamical cores, in: P.H. Lauritzen, R.D. Nair, C. Jablonowski, M. Taylor (Eds.), Numerical techniques for global atmospheric models. *Lecture Notes in Computational Science and Engineering, Springer*, 80.

Whitehead, J., Jablonowski, C., Rood, R. B., and Lauritzen, P. H. (2011). A stability analysis of divergence damping on a latitude-longitude grid. *Mon. Wea. Rev.*, 139:2976–2993.

Williamson, D. L. (2002). Time-split versus process-split coupling of parameterizations and dynamical core. *Mon. Wea. Rev.*, 130:2024–2041.

Williamson, D. L. and Olson, J. G. (2003). Dependence of aqua-planet simulations on time step. *Quart. J. Roy. Meteor. Soc.*, 129(591):2049–2064.

Zarzycki, C. M., Jablonowski, C., and Taylor, M. A. (2014). Using variable-resolution meshes to model tropical cyclones in the community atmosphere model. *Mon. Wea. Rev.*, 142(3):1221–1239.